

RhoJ is an endothelial cell-restricted Rho GTPase that mediates vascular morphogenesis and is regulated by the transcription factor ERG

Lei Yuan,¹⁻³ Anastasia Sacharidou,⁴ Amber N. Stratman,⁴ Alexandra Le Bras,¹⁻³ Peter J. Zwiers,⁵ Katherine Spokes,^{2,3} Manoj Bhasin,⁶ Shou-ching Shih,^{3,7} Janice A. Nagy,^{3,7} Grietje Molema,⁵ William C. Aird,^{2,3} George E. Davis,^{4,8} and Peter Oettgen¹⁻³

¹Division of Cardiology, ²Division of Molecular and Vascular Medicine and Department of Medicine, Beth Israel Deaconess Medical Center, Harvard Medical School, Boston, MA; ³Center for Vascular Biology Research, Beth Israel Deaconess Medical Center, Harvard Medical School, Boston, MA; ⁴Department of Medical Pharmacology, School of Medicine and Dalton Cardiovascular Sciences Center, University of Missouri-Columbia, Columbia, MO; ⁵Department of Pathology and Medical Biology, Medical Biology Section, University Medical Center Groningen, University of Groningen, Groningen, The Netherlands; ⁶Division of Interdisciplinary Medicine and Biotechnology, Beth Israel Deaconess Medical Center, Harvard Medical School, Boston, MA; ⁷Department of Pathology, Beth Israel Deaconess Medical Center, Harvard Medical School, Boston, MA; and ⁸Department of Physiology and Pathology and Anatomical Sciences, School of Medicine and Dalton Cardiovascular Sciences Center, University of Missouri-Columbia, Columbia, MO

ERG is a member of the ETS transcription factor family that is highly enriched in endothelial cells (ECs). To further define the role of ERG in regulating EC function, we evaluated the effect of ERG knockdown on EC lumen formation in 3D collagen matrices. Blockade of ERG using siRNA completely interferes with EC lumen formation. Quantitative PCR (QPCR) was used to identify potential downstream gene targets of ERG. In particular,

we identified RhoJ as the Rho GTPase family member that is closely related to Cdc42 as a target of ERG. Knockdown of ERG expression in ECs led to a 75% reduction in the expression of RhoJ. Chromatin immunoprecipitation and transactivation studies demonstrated that ERG could bind to functional sites in the proximal promoter of the RhoJ gene. Knockdown of RhoJ similarly resulted in a marked reduction in the ability of ECs to

form lumens. Suppression of either ERG or RhoJ during EC lumen formation was associated with a marked increase in RhoA activation and a decrease in Rac1 and Cdc42 activation and their downstream effectors. Finally, in contrast to other Rho GTPases, RhoJ exhibits a highly EC-restricted expression pattern in several different tissues, including the brain, heart, lung, and liver. (*Blood*. 2011; 118(4):1145-1153)

Introduction

Blood vessel lumenization is a critical step in the development of a functional vascular system during vascular morphogenesis.^{1,2} Major mechanisms of lumen formation include cell wrapping, budding, cavitation, cord hollowing, and cell hollowing.³ Recently, there have been significant advances in our understanding of how endothelial cells (ECs) make lumens and tubes in 3D extracellular matrices.^{4,5} We have shown that this process is regulated by the formation of intracellular vacuoles within ECs that aggregate and coalesce.⁶ EC lumen and tube expansion occurs through MT1-MMP (membrane type 1-matrix metalloprotease)-dependent proteolysis of 3D collagen matrices. One of the key regulators of lumen formation is the Rho GTPase Cdc42, which was first shown to control this process in ECs and later in epithelial cells.⁶⁻⁹ During EC tube formation, Cdc42 activates a signaling cascade that includes PKC ϵ , p21 protein-activated kinase Pak2, Pak4, Src-family kinases (SFKs) Src, Yes, B-Raf, C-Raf, and ERK1/2.¹⁰ Other Rho GTPases that have recently been evaluated for their role in EC tube formation include RhoA and Rac1.⁵ Whereas knockdown of Rac1 with siRNA markedly inhibits EC lumen formation, suppression of RhoA has no effect.

The ETS factors are a family of approximately 30 transcription factors that share a highly conserved DNA-binding domain.¹¹ ETS factors were originally identified as playing a central role in

regulating several B- and T-cell-specific genes involved in hematopoiesis. We and others have also demonstrated a critical role for selected ETS family members in the regulation of several vascular specific genes, including Tie1, Tie2, VWF, Robo4, and endothelial nitric oxide synthase.¹²⁻¹⁶ Although many ETS factors participate in the regulation of EC-restricted genes, most do not exhibit a vascular-specific expression pattern. However, several recent studies—including those from our own laboratory—have shown that the ETS factor ERG exhibits an EC-restricted expression pattern.¹⁷⁻²⁰ Furthermore, it has also been shown that several EC-restricted genes, including VE-cadherin, endoglin, and VWF, are regulated by ERG.²¹⁻²³ In addition to its function as a regulator of EC-specific gene expression, ERG also plays a developmental role during the differentiation of embryonic stem cells into ECs.^{24,25}

More recently, ERG has been shown to play a role in endothelial tube formation and angiogenesis.²¹ In particular, one of the main downstream targets of ERG identified as playing a role in this process was VE-cadherin. The purpose of this study was to further define the regulatory role of ERG during EC morphogenesis. We found a dramatic inhibitory effect on EC tube and lumen formation in 3D collagen gels as a result of siRNA suppression of ERG. Using quantitative PCR (QPCR) of potential candidate genes we were able to identify the Rho GTPase family member, RhoJ, which is

Submitted October 25, 2010; accepted May 15, 2011. Prepublished online as *Blood* First Edition paper, May 31, 2011; DOI 10.1182/blood-2010-10-315275.

The publication costs of this article were defrayed in part by page charge payment. Therefore, and solely to indicate this fact, this article is hereby marked "advertisement" in accordance with 18 USC section 1734.

The online version of this article contains a data supplement.

© 2011 by The American Society of Hematology

closely related to Cdc42, as a novel downstream target of ERG. In contrast to other Rho GTPases, RhoJ exhibits a highly EC-restricted expression pattern that is similar to the ETS factor ERG and knock-down of RhoJ in ECs similarly blocks EC tube morphogenesis in 3D matrices. Adenoviral expression of RhoJ in ERG siRNA-treated ECs partially rescued the ability of ECs to form lumens in 3D collagen matrices.

Methods

Luciferase reporter gene constructs

Human RhoJ promoter (−1184 to +142 bp) fragments were cloned from genomic DNA freshly extracted from HUVECs using 2-step PCR. The first step used outside primers hRhoJ-out-F and hRhoJ-out-R, followed by PCR using nested primers hRhoJ-nest-F and hRhoJ-nest-R (sequences are shown in supplemental Table 3, available on the *Blood* Web site; see the Supplemental Materials link at the top of the online article), each of which contains *KpnI* and *XhoI* cutting sites, respectively. This 1326-bp fragment was inserted into the *KpnI-XhoI* site and subcloned into the pGL3 basic luciferase reporter vector (Promega).

Laser capture microdissection

Five 9- μm cryosections mounted on 1.35- μm polyethylene-naphthalene membranes (P.A.L.M.; Microlaser Technology) were fixed in acetone and stained with Mayer hematoxylin, washed with diethyl pyrocarbonate-treated water, and air-dried. ECs from arterioles and venules, as well as the endocard, were dissected using the LMD6500 microdissection system (Leica Microsystems). All vascular structures were histologically identified, selected, and dissected at a 200 \times magnification. For the endocard, an area of $1.5 \times 10^6 \mu\text{m}^2$ was microdissected; for small arterioles, an area of $\sim 7 \times 10^5 \mu\text{m}^2$ was dissected; and for venules, an area of $\sim 1.3 \times 10^6 \mu\text{m}^2$ was dissected (all areas consisting of lumen and cells). To discriminate arterioles from venules, we were guided by endomucin staining of sequential slides in which arterioles showed up negative (supplemental Figure 9A). The anti-endomucin Ab was kindly provided by Dr Dietmar Vestwebe (Munster, Germany). To obtain the capillaries, 9- μm cryosections were mounted on 1.4- μm polyethylene-terephthalate FrameSlides (Leica Microsystems). Before laser microdissection, tissues were fixed in acetone and immunofluorescently stained with Fluorescein *Griffonia (Bandeiraea) simplicifolia* Lectin I Isolectin B4 (Vector Laboratories; supplemental Figure 9B). The area of dissected capillaries was $\sim 6 \times 10^5 \mu\text{m}^2$. Extraction of total RNA from the dissected materials was carried out according to the protocol with the RNeasy Micro Kit (QIAGEN).

EC lumen and tube formation in 3D collagen matrices

For vasculogenic assays, HUVECs were suspended as single cells within 3.75 mg/mL collagen type I matrices and allowed to undergo EC morphogenesis using our microassay system as described previously.^{6,7} Cultures were fixed at the indicated time points with 3% glutaraldehyde and stained with toluidine blue before photography by light microscopy. Visualization and image acquisition of EC lumen formation was performed using an inverted microscope (CKX41; Olympus). Image analysis was performed using MetaMorph software. EC lumen formation was quantitated by tracing luminal areas using MetaMorph software, as described previously.^{6,7}

3D EC culture pull-down assays for components of the lumen signaling complex

Adenovirus infection of ECs was performed as described previously.^{6,7} Infected ECs were suspended within 3.75 mg/mL of collagen type I matrices and allowed to undergo morphogenesis for 24 hours. 3D gels were extracted to examine protein expression or used to examine activation of Rho GTPases and protein-protein interactions. MT1-MMP-s wt, Jam B-s wt, and S-GFP-Cdc42 were amplified from human cDNA clones (Origene)

and were constructed as described previously.^{6,7} EC lumen formation assays were established as described previously^{6,7} using ECs expressing S-tag containing or control recombinant proteins. Cultures were lysed at the indicated time points using cold detergent lysis buffer made of 1% Triton X-100 in 1 \times TBS, pH 8.0, containing 150 $\mu\text{g}/\text{mL}$ of high-purity collagenase (Sigma-Aldrich), 100nM GTP γS (EMD), and complete EDTA-free protease inhibitor cocktail tablets (Roche). Lysates were incubated at 4°C for 1 hour for collagen to be digested, and then were clarified by centrifugation at 22 000g for 20 minutes at 4°C. Supernatants were then collected and precleared using glycine-Sepharose 4B beads (Sigma-Aldrich) for 2 hours at 4°C. At the end of incubation, samples were mildly centrifuged for 30 seconds to pellet the beads. Supernatants were then collected and incubated with S-protein agarose (Novagen) for 90 minutes at 4°C. After washing 3 times, the bound proteins were detected by Western blot analysis.

GTPase activity assay in 3D gel

GTPase assays were performed at 16 hours during the tubulogenic process in 3D collagen gels. ECs were suspended at 2×10^6 cells/mL in defined serum-free media conditions as we have described previously.¹⁰ For each condition, 20 collagen gels (total of 10^6 cells) were harvested using a detergent lysis buffer that was optimized for RhoGTPase activity assays in our systems.¹⁰ Cultures were lysed as described previously. Supernatants were incubated with GST-PAK-PBD or GST-RhoA-PBD protein beads for 90 minutes at 4°C to assess the degree of Cdc42, Rac1, or RhoA activation.^{6,7} The beads were washed 4 times with washing buffer containing 0.1% Triton X-100 in 1 \times TBS, pH 8.0. Bound MT1-MMP-, Jam B-, and Cdc42-associated proteins such as RhoJ were detected by Western blot analysis. All bound active Cdc42, Rac1, or RhoA proteins were also detected by Western blots.

Generation of RhoJ adenovirus

The human RhoJ cDNA was obtained using a nested PCR strategy. HUVEC cDNA was used as a template and following primers were used: hRhoJ-cDNA-F and hRhoJ-cDNA-R, and for the nested PCR the hRhoJ-cDNA-nest-F and hRhoJ-cDNA-nest-R. The hRhoJ cDNA was then digested with *EcoRI* and *BamHI* restriction enzymes and inserted in the *EcoRI/BamHI* sites of the phrGFP II-N vector (Stratagene) to generate the phrGFP II-N-RhoJ plasmid. The GFP-II-N-hRhoJ insert was then PCR amplified from the phrGFP II-N-RhoJ plasmid using the primers hRhoJ-phrGFP-F and hRhoJ-phrGFP-R. The primer sequences are included in supplemental Table 3. The PCR product was then digested with the restriction enzymes *SalI* and *EcoRV* and inserted in the *SalI/EcoRV* sites of the pCMV shuttle vector. Standard restriction digestion cloning was performed to clone it into the pAdShuttle-CMV vector. Positive clones were confirmed by sequencing. Recombination of the positive clones and virus production were carried out as described previously.²⁶ The adenovirus propagation protocol used has also been described previously.⁶ Protein expression of RhoJ by each of the adenoviral constructs was confirmed by Western blot analysis.

EC/pericyte coculture

ECs (at 2×10^6 cells/mL) were treated with luciferase control siRNA or with siRNAs to ERG or RhoJ, and then suspended with human brain vascular pericytes (0.4×10^6 cells/mL; ScienCell) in 2.5 mg/mL of collagen type I matrices and incubated at 37°C in culture medium containing reduced serum supplement and FGF-2 at 40 ng/mL. SCF, stromal-derived factor-1 (SDF-1), and IL-3 were added at a 200 ng/mL concentration into the collagen type I matrix as described previously.²⁷ These cultures were allowed to assemble over 72 hours and then fixed with 3% glutaraldehyde to be processed for further analysis.

EC siRNA transfection followed by adenovirus infection for rescue experiments

EC transfection of siRNAs for RhoJ, ERG, and luciferase control was carried out in growth medium with 1% serum as described previously.⁷ At the end of the siRNA transfection protocol, ECs were transfected with

adenoviruses expressing GFP-RhoJ, ERG, and green fluorescent protein (GFP) used as a control. Infected ECs were allowed to express the recombinant protein of interest overnight and then were suspended, as single cells, in 3.75 mg/mL collagen as described previously.⁷ Cultures were fixed after 24 hours with 3% glutaraldehyde, stained, and photographed. Lumen areas were quantitated by tracing photographs using MetaMorph Version 7.7.2. software.

Statistical analysis

Statistical analysis of EC vasculogenesis was performed using SPSS 11.0 software. Other statistics were assessed by a paired-samples *t* test. A value of *P* < .05 was considered significant.

Results

ERG is required for EC lumen and tube formation in 3D collagen matrices

ERG is an EC-enriched ETS factor that has been shown previously to regulate several EC-restricted genes. We have previously tested 4 independent ERG siRNAs (1-4) to knock down ERG compared with control siRNA (CTR) in HUVECs using Western blot analysis.²⁰ Eighty to 90% reductions in ERG protein levels were observed with siRNA 2 and 4, respectively, whereas only ~ a 60% reduction was observed with ERG siRNA 3 (data not shown). To ensure the specificity of the ERG siRNA, we previously examined the expression levels of a panel of other ETS factors, including Ets-1, Ets-2, Fli-1, Ets-1, ELF-1, and Nerf1, before and after ERG siRNA treatment. No change in the expression of any of the other ETS factors except ERG was observed after ERG siRNA treatment.²⁰ ERG siRNAs 2 and 4 significantly blunted EC lumen and tube formation compared with control siRNA (Figure 1A). It has been shown previously that suppression of ERG leads to EC apoptosis.²¹ This represents at least one potential mechanism by which suppression of ERG could lead to decreased EC tube and lumen formation. Quantitation of lumen and vessel area confirmed the marked reduction in EC lumens and tubes that formed in the presence of ERG siRNA (Figure 1A). The accompanying videos more clearly demonstrate the significant reductions in the ability of ECs to form tubes and lumens over time in the presence of ERG siRNA (supplemental Videos 1-2). We next examined the ability of ERG siRNA to interfere with the formation of branching tubular structures using ECs alone or in combination with pericytes (Figure 1B) and ERG siRNA significantly reduced tube formation in both circumstances.

Identification of novel ERG target in vascular morphogenesis

To identify potential downstream targets of ERG that may be involved in vascular morphogenesis, we analyzed the expression of several genes that we and others have shown previously to be involved in the regulation of EC morphogenesis in HUVECs treated with ERG siRNA compared with control siRNA.^{6,7} QPCR was used to quantify the changes in expression of the selected genes (supplemental Figure 1). Of particular interest to us was a marked reduction in the Cdc42-related Rho GTPase family member RhoJ (also known as TCL) as a result of ERG siRNA treatment. In contrast to RhoJ, there was no significant change in the expression of other Rho GTPase family members, including RhoA, Rac1, Cdc42, and TC10 (also known as RhoQ). A modest (20%-30%) reduction in JamB, Pak2, VE-cadherin, and Par3 was observed. Interestingly, all 4 of these latter genes have been shown

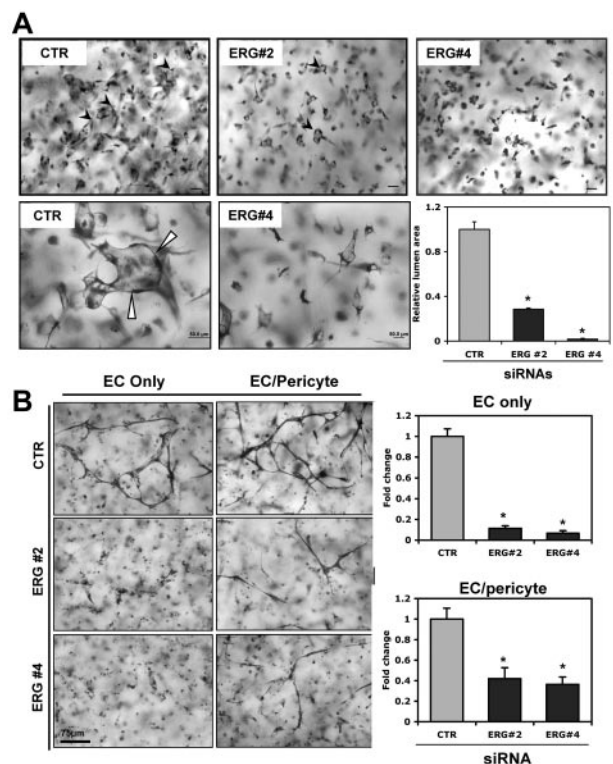


Figure 1. ERG knock-down blocks EC lumen and tube formation in 3D collagen matrices. ECs were treated with single siRNAs targeting ERG (siRNAs 2 and 4; 40 nmol/L) or control (40 nmol/L) and incubated for 24 hours. (A) Transfected HUVECs were seeded as single cells in 3D collagen type I matrices (at 2×10^6 cells/mL) to undergo lumen formation for 24 hours before preparation of fixation, staining, and photography. Representative fields of siRNA-treated ECs from lumen formation are shown as both lower- (top) and higher-powered (bottom) images. Arrows indicate EC lumens. EC luminal areas were quantitated using MetaMorph software. Data shown are presented as normalized values of lumen area per high powered field relative to control (CTR) treatment \pm SD, *n* = 20, *P* < .01. (B) Transfected HUVECs were seeded in 3D collagen matrices in the presence (EC/pericyte) or absence (EC only) of pericytes to undergo tube morphogenesis for 72 hours. Quantitation of relative vessel area was done on ERG suppression versus control conditions. Data shown are presented as normalized values of lumen area per high powered field relative to control treatment \pm SD, *n* = 20, *P* < .01.

to control EC tube morphogenesis in 3D matrices.^{7,28,29} To further validate the dependency of RhoJ on ERG expression, we tested 4 independent siRNAs directed against ERG and observed similar reductions in RhoJ expression at the level of mRNA (Figure 2A). Western blot analysis was used to evaluate the corresponding reduction in RhoJ protein for one of the ERG siRNAs (Figure 2B). These results support the idea that ERG regulates the expression of several genes, and in particular RhoJ, that are involved in controlling the formation of EC tubes.

RhoJ is a direct transcriptional target of ERG

To evaluate whether RhoJ is a direct target of ERG, we subcloned 1.3 kb of the proximal promoter of the human RhoJ gene into the pGL3 luciferase reporter. We identified 3 highly conserved binding sites (-44, -30, and -8) for ERG in the proximal 100 bp of the RhoJ promoter (Figure 2C). Cotransfections in HUVEC cells using the RhoJ promoter construct and expression plasmids encoding ERG or a control plasmid demonstrated a significant dose-dependent increase (~ 5-fold) in RhoJ promoter activity with the ERG expression plasmid compared with the control plasmid (Figure 2D). We next evaluated the ability of a panel of ETS factors to transactivate the RhoJ promoter, and only ERG potently transactivated the promoter (Figure 2E). The ChIP assay was used

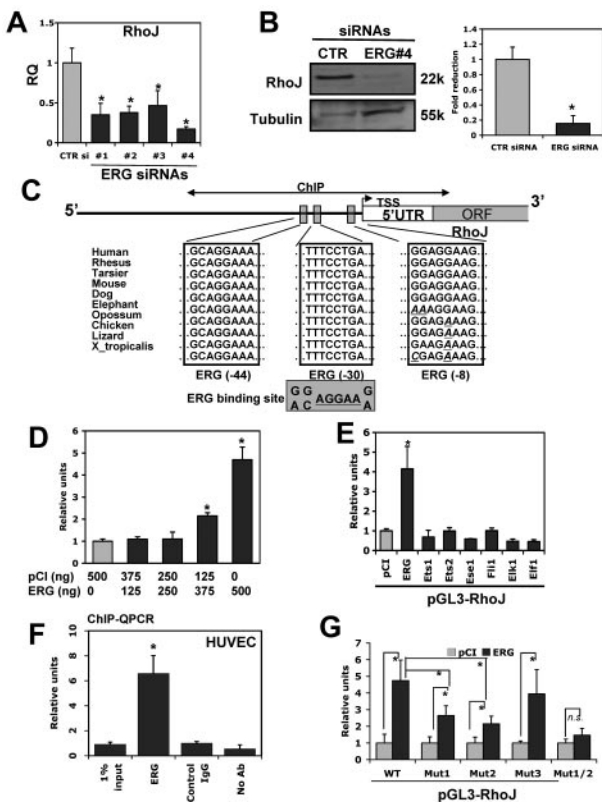


Figure 2. RhoJ is a novel target of ERG that is implicated in EC lumen formation. HUVECs were transfected with indicated siRNA (40 nmol/L). After 48 hours of incubation, RNA was extracted for QPCR. (A) Evaluation of RhoJ expression at the RNA level in ERG siRNA-treated HUVECs. HUVECs were transfected with ERG siRNA 1-4 or nontargeting control siRNA (40 nmol/L). The mRNA levels of RhoJ within the same samples were assessed by QPCR using specific primers for RhoJ. TATA-box binding protein was used as internal control for normalization ($n = 3$). $*P < .05$. (B) Cell extracts were prepared from HUVECs transfected with either nontargeting control siRNA or ERG siRNA 4 (40 nmol/L). Equal amounts of total proteins were separated on PAGE gel. Protein levels of RhoJ and the loading control tubulin were determined by Western blot analysis. Representative Western blot analysis shows protein bands of RhoJ and tubulin. Quantitation was done by densitometric analysis ($n = 3$). $*P < .05$. (C) Schematic diagram of ERG-binding sites within the proximal promoter of the RhoJ gene. The 1.3-kb upstream promoter region of RhoJ was analyzed for putative ERG-binding site based on the known ERG consensus-binding site derived from previously characterized ERG target genes. Blue boxes indicate the putative ERG-binding sites. The bidirectional arrows marked the target regions for ChIP assays. (D-E) HUVECs were cotransfected with RhoJ promoter luciferase reporter and pCI expressing vector encoding indicated cDNA for selected ETS factors or the empty vector. After 24 hours of incubation, cells were lysed and cell lysates were analyzed for luciferase activity. The data are shown as relative luciferase activity compared with cotransfection with empty expression plasmid. (F) ChIP assay of the proximal RhoJ promoter using HUVECs. An ERG polyclonal Ab was used to precipitate the cross-linked DNA. QPCR analysis of the input in the absence of any IgG (no-Ab) and in the presence of nonspecific normal IgG (control IgG) or ERG antibody (ERG) after immunoprecipitation (IP) was performed using PCR primers corresponding to the region encoding 3 ERG putative binding sites within the proximal RhoJ promoter. The data are presented relative to control IgG. (G) Promoter transactivation assays were repeated by cotransfecting pCI-ERG with either RhoJ mutants or the wild-type promoter. The results are shown relative to control pCI-treated samples ($n = 3$). $*P < .05$.

to determine whether ERG physically binds to one of the 3 conserved ERG-binding sites in the proximal RhoJ promoter. ERG was shown to bind with high affinity to this region compared with the control (Figure 2F). To evaluate the functional role of the -44, -30, and -8 ERG-binding sites in the transactivation of the RhoJ promoter by ERG, we generated point mutations of the RhoJ promoter. The resulting constructs were transiently transfected into HUVECs along with the ERG expression plasmid (Figure 2G). Mutation of the -44 (Mut1) or -30 (Mut2) ERG sites resulted in

significant reduction of RhoJ promoter activity (44% and 54%, respectively; Figure 2G) compared with the wild-type promoter. In contrast, mutation of the -8 site (Mut3) did not alter the promoter activity. We also generated double mutants (Mut1/2) within both the -44 and -30 ERG-binding sites that completely abolished the ability of ERG to transactivate the RhoJ promoter. These results suggest that 2 of the 3 ERG-binding sites (-44 and -30) coordinately function to mediate RhoJ expression by ERG in ECs. Mutation of these 2 sites also reduced the basal activity of the promoter in ECs (supplemental Figure 2).

RhoJ knock-down blocks EC lumen formation

We also sought to determine whether knock-down of RhoJ leads to similar phenotypic changes in ECs during lumen formation in collagen matrices as knock-down of ERG. The knock-down efficiency of RhoJ siRNAs is shown in Figure 3A-B at the level of RNA and protein, with RhoJ siRNA 3 leading to an ~90% reduction in RhoJ whereas siRNA 2 reduced RhoJ protein levels by approximately 75%. Interestingly, knock-down of RhoJ blocked lumen formation significantly in 3D collagen matrices (Figure 3C and supplemental Videos 1,3-4) in a similar fashion as ERG siRNA. RhoJ siRNA also inhibited the formation of EC tubes and branching structures when combined with pericytes (Figure 3D). We quantitatively compared the relative lumen area in 3D collagen gels over time in control siRNA-, RhoJ siRNA-, and ERG siRNA-treated ECs (Figure 3E). ERG siRNA was a somewhat more potent inhibitor of tube formation. We next tested the ability of RhoJ siRNA to block EC cord formation in a 2D matrigel assay. EC cord formation was significantly blocked by RhoJ siRNA in this assay (supplemental Figure 3). Finally, we evaluated the ability of RhoJ siRNA to inhibit angiogenesis in vivo using a modification of the Matrigel assay described previously.²¹ A mixture containing Matrigel, 2 μ M siRNA, basic FGF, and heparin was injected subcutaneously into nude mice and harvested, fixed in 4% paraformaldehyde, paraffin embedded, and processed for staining. The animal experiments were approved by the institutional review board of Beth Israel Deaconess Medical Center. We observed a significant reduction in the number of blood vessels that formed in the RhoJ siRNA-treated Matrigel plugs compared with the controls, as determined by H&E and CD31 staining (Figure 4).

It has been shown previously that transfection of ECs to ERG siRNA leads to an increase in apoptosis compared with control siRNA.²¹ We also tested the effect of RhoJ siRNA on EC apoptosis using the terminal deoxynucleotidyltransferase-mediated dUTP nick end-labeling stain assay. RhoJ siRNA did not lead to significant EC apoptosis (supplemental Figure 4), suggesting that the mechanism by which ERG suppression leads to EC apoptosis is independent of RhoJ.

Partial rescue of ERG siRNA-treated ECs by adenoviral delivery of RhoJ

We next evaluated the ability of an adenovirus expressing RhoJ to rescue ECs treated with RhoJ siRNA or ERG siRNA compared with control siRNA-treated cells (Figure 5A-B). A GFP-expressing adenovirus was used as a control. The RhoJ adenovirus had no effect on tube formation in control siRNA-treated cells, but not unexpectedly was able to fully rescue the RhoJ siRNA-treated ECs. Of particular interest to us was that the RhoJ adenovirus was able to rescue ERG siRNA-treated ECs by 62%, supporting the concept that RhoJ is a major downstream target of ERG that is involved in EC lumen formation. The overexpression of the

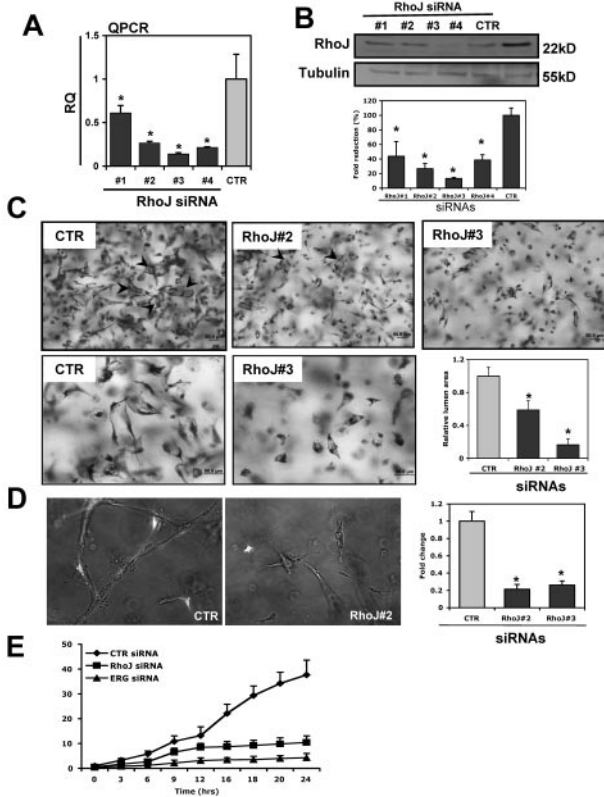


Figure 3. RhoJ knock-down blocks EC lumen formation. (A-B) The ability of RhoJ siRNA to repress RhoJ expression. HUVECs were transfected with various RhoJ siRNAs (siRNAs 1-4; 40 nmol/L) or a control siRNA (CTR). After incubation for 48 hours, RhoJ expression was assessed by QPCR using RhoJ-specific primers (A) or by Western blot analysis using anti-RhoJ antibody (B). Tubulin was used as a loading control. Quantitation was done by densitometric analysis (n = 3). *P < .05. (C) ECs were treated with RhoJ siRNAs 2 and 3 (40 nmol/L). After incubation for 24 hours, cells were seeded as single cells in 3D collagen type I matrices for 24 hours before preparation of fixation, staining, and photography. EC luminal areas were quantitated using Metamorph software. Data shown are presented as values of normalized lumen area per high powered field relative to control samples ± SD, n = 20, *P < .01. Representative images of both lower- (top) and higher-powered (bottom) from lumen formation in siRNA-treated ECs are shown. Arrows indicate EC lumens. (D) RhoJ (siRNAs 2 and 3) or control siRNA (40 nmol/L) transfected HUVECs were seeded in 3D collagen matrices in the presence of pericytes to undergo tube morphogenesis as described above. Green colored cells are pericytes. Quantitation of relative vessel area was done on RhoJ suppression versus control conditions. Data shown are presented as normalized values of lumen area per high powered field relative to control treatment ± SD, n = 20, *P < .01. (E) Temporal analysis of EC tubulogenesis following siRNA suppression of ERG and RhoJ. ECs were first treated with control (CTR), ERG siRNA 4 and RhoJ siRNA 3 (40 nmol/L). After 24 hours of incubation, the lumen area was quantitated over 24 hours from time-lapse videos (see supplemental Videos 1-4). Data are shown as average EC luminal area per high powered field relative to control ± SD, n = 5, P < .01.

GFP-RhoJ fusion protein delivered in adenovirus was confirmed by Western blot analysis (Figure 5C).

Rho GTPase activation by RhoJ knock-down during EC lumen formation

Because RhoJ and ERG appear to be critical regulators of EC lumen formation, we next determined whether the levels of either of these proteins changes in ECs during lumen formation. We did not observe significant changes in the expression levels of either protein over a 48-hour period (supplemental Figure 5A). Because RhoJ is most closely related to Cdc42, we investigated whether RhoJ could physically interact with Cdc42 or possibly one of its effectors. To that end, we used a recombinant virus containing Cdc42 tagged with both an N-terminal GFP and an S tag. ECs were

infected with S-GFP-Cdc42 or control GFP viruses for 24 hours before they were suspended within 3D collagen matrices. EC extracts were prepared at 16 hours and lysates were incubated with S-protein agarose beads to capture the recombinant Cdc42. RhoJ strongly associated with Cdc42 and not with the GFP control. Weaker but detectable interactions were observed between RhoJ and JamB or MT1-MMP (Figure 6A), which are known to co-associate in multiprotein complexes that regulate lumen formation.²⁸ These results support the concept that RhoJ interacts with Cdc42 (or a binding partner of Cdc42) to participate in a multiprotein complex with several other proteins to control EC morphogenesis.

It has been shown previously that EC lumen formation is associated with activation of Rac1 and Cdc42, as well as downstream effectors. We were therefore interested in evaluating whether knock-down of ERG or RhoJ affects Rho GTPase activation during the process of lumen formation in 3D collagen matrices. We observed that siRNA suppression of both RhoJ and ERG significantly blunted Rac1 activation without affecting the total levels of Rac1 (Figure 6B; supplemental Figure 5B). Similarly, there was a modest reduction in Cdc42 activation. In contrast, knock-down of ERG and RhoJ led to a dramatic increase in RhoA activation with no change in total RhoA levels. Interestingly, previous studies have shown that RhoA controls EC tube collapse in 3D matrices.³⁰

Among the diverse number of Rho GTPase targets, Pak proteins are known to be critical downstream effectors that regulate cytoskeletal function.³¹ We have shown that 2 members of the Pak family are required for EC lumen formation in 3D collagen matrices.^{5,7} More recently, we have shown that Cdc42-dependent

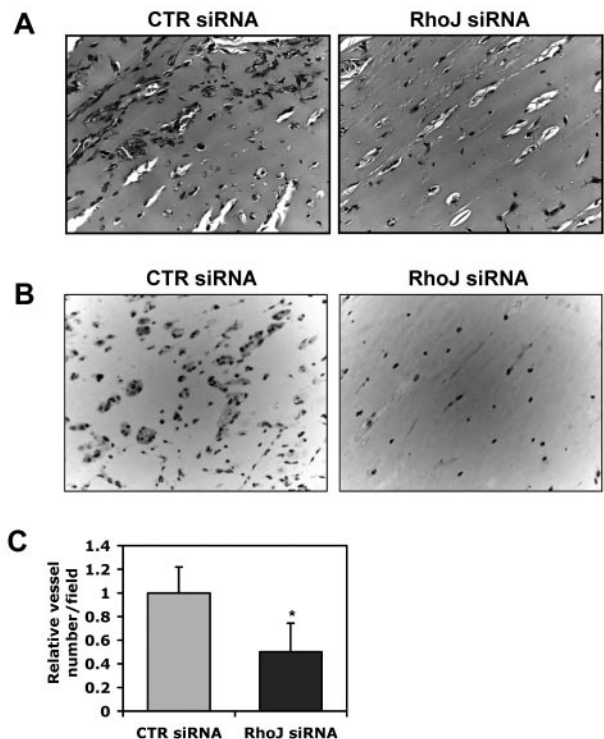


Figure 4. Effects of RhoJ on tube formation in Matrigel in vivo. Matrigel mixture containing 2µM control or RhoJ siRNA was injected subcutaneously into nude mice. The gel plugs were collected after 7 days. After fixation in paraffin, samples were embedded in paraffin, sectioned and H&E stained. (A) Representative images from H&E staining. (B) Representative images of immunohistochemistry staining using CD31 antibody. (C) The quantitative data are shown as the number of vessels containing red blood cells relative to the control condition (n = 5).

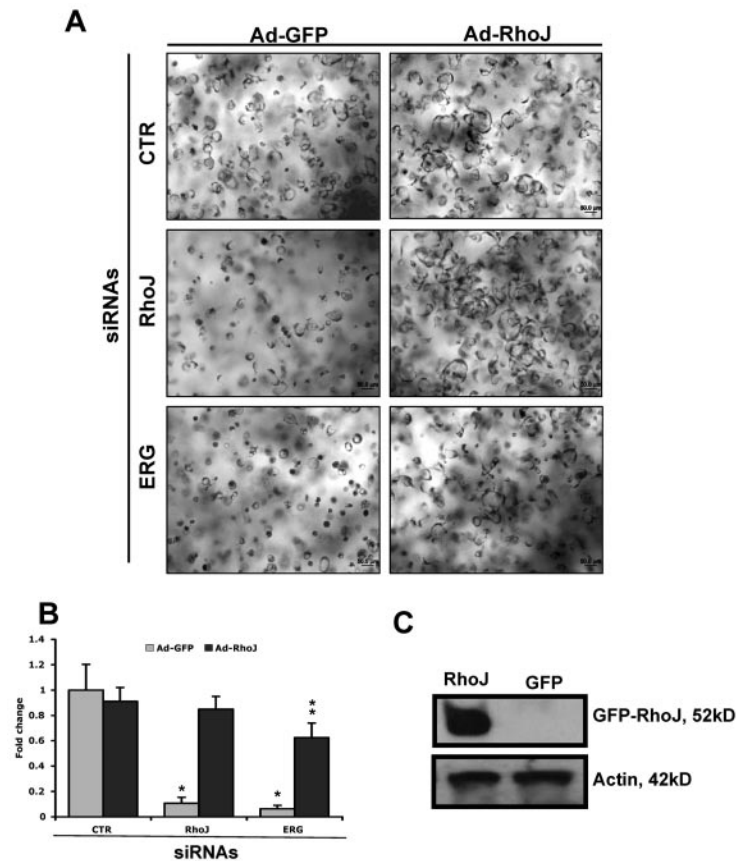


Figure 5. Partial rescue of ERG siRNA effects on EC lumen and tube formation by adenoviral delivery of RhoJ. (A-B) HUVECs were first transfected with ERG, RhoJ, or control siRNA (40 nmol/L) before infection with adenovirus encoding either GFP or RhoJ as indicated. ECs were then seeded in 3D collagen matrices for 24 hours. Lumen area was quantitated using Metamorph software and is presented relative to lumen area obtained for the control GFP adenovirus. *Comparison with CTR siRNA-treated EC. **Comparison with Ad-GFP infected EC with the same siRNA treatment. (C) ECs were infected with adenovirus encoding either GFP or RhoJ. The expression of GFP-RhoJ fusion protein was detected by Western blot using anti-RhoJ antibody and actin as a loading control.

EC lumen formation involves the coordinated signaling of PKC ϵ together with the SFKs Src and Yes, leading to the activation of Pak2 and Pak4. Pak2 and Pak4 further activate 2 Raf kinases, B-Raf and C-Raf, leading to ERK1 and ERK2 (ERK1/2) activation. Knock-down of RhoJ and ERG significantly decreased the phosphorylation of Pak2 and Pak4 at the 24-hour point during EC lumen formation (Figure 6C and supplemental Figure 6). Similarly, phosphorylation of B-Raf was also diminished after knock-down of RhoJ and ERG. These overlapping results suggest that RhoJ is a major downstream target of ERG. Interestingly, knock-down of ERG also significantly diminished phosphorylation of C-Raf and Src family members, whereas knock-down of RhoJ had only a mild to modest effect on phosphorylation of these proteins, suggesting that ERG must affect the expression of other proteins involved in regulating the activation of these proteins.

RhoJ is highly enriched in ECs

Most of the Rho GTPases are widely expressed in many cell types and tissues, playing important roles in a variety of cellular functions. Previous studies have not evaluated the relative expression of the Rho GTPases in ECs compared with other cell types. Given the fact that ERG is highly expressed in ECs and our findings of RhoJ as a direct target of ERG, we wondered whether RhoJ might also exhibit a similar expression pattern. Interestingly, RhoJ has an expression pattern that is distinct from other Rho GTPases. It is highly enriched in all ECs, including arterial, venous, and microvascular ECs, with low levels of expression in aortic smooth muscle cells, and was barely detectable in all other cell types we examined (Figure 7A). A similar pattern of expression was observed in murine cells (Figure 7B). RhoJ was highly expressed in

primary ECs isolated from mouse heart and lung, as well as the EC cell lines PY41, bEND, and MS1. We also evaluated the expression of other Rho GTPases, including RhoA, RhoB, Rac1, RhoG, Cdc42, and TC10, in a variety of human ECs and non-ECs (supplemental Figure 7). Of the Rho GTPases, RhoJ exhibited the most EC-restricted pattern of expression, whereas other Rho GTPases were expressed in several non-EC cell types.

RhoJ expression in tissues

RhoJ expression was also evaluated by immunofluorescence in various mouse tissues including heart, brain, and liver (Figure 7C and supplemental Figure 8). These studies demonstrated a close association between RhoJ expression and cells expressing the EC-specific marker CD31. 4',6-Diamidino-2-phenylindole, dihydrochloride (DAPI) staining showed many cells that did not express either gene. QPCR was used to evaluate the relative expression of RhoJ in different tissues, including the brain, lung, heart, liver, and kidney (Figure 7D). RhoJ expression was highest in the heart and lung. Additional studies evaluating the expression of RhoJ in a variety of vascular beds suggest that there is marked heterogeneity in the distribution of RhoJ gene expression in different ECs. To further define the heterogeneity of RhoJ in different types of ECs in the heart, including endocardial, arterial, venular, and capillary ECs, we used laser microdissection (LMD) to isolate different heart ECs (supplemental Figure 9).^{32,33} To assess the ability of our LMD approach of isolating ECs in the heart to evaluate heterogeneity in EC expression, we compared the relative expression of some commonly known EC markers using both QPCR and immunohistochemistry. The immunohistochemistry staining corroborated our findings from QPCR (data not shown).

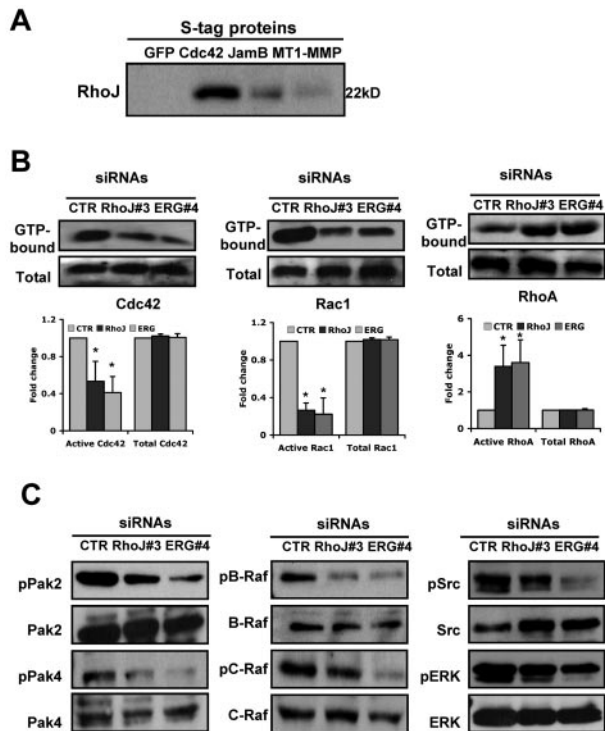


Figure 6. ERG and RhoJ siRNA knock-down markedly inhibit Rac-1 and Cdc42 Rho GTPase activation, whereas RhoA activation is strongly increased during EC lumen formation in 3D collagen matrices. (A) ECs were infected with recombinant adenoviruses carrying S-epitope-tagged GFP-Cdc42, JamB, and MT1-MMP or GFP as a control. EC cultures in 3D matrices were prepared and after 16 hours, lysates were prepared and incubated with S-protein beads. Beads were eluted with SDS-PAGE sample buffer and samples were run on gels and Western blots probed with antibody against RhoJ. (B) Cultures were established as described in "Methods," and after 16 hours, detergent lysates were prepared to assess the degree of Cdc42, Rac1, and RhoA activation. Starting material lysates and the eluates from the Pak and Rhotekin beads were assessed by Western blots using anti-Cdc42, anti-Rac1, and anti-RhoA antibodies. Representative images are shown (additional ones are included in supplemental Figure 5B). Quantitation was done by densitometric analysis ($n = 3$). $*P < .01$. (C) ECs were treated with the indicated siRNAs (40 nmol/L) for ERG and RhoJ, and 24 hours later, were seeded within 3D collagen matrices to undergo morphogenesis. After 24 hours of culture, EC lysates were prepared and analyzed for the indicated molecules. In each case, we analyzed for phosphorylated kinases as an indicator for kinase activation, as well as the total levels of each kinase.

Finally, we evaluated the expression of ERG and RhoJ in the different types of heart ECs (Figure 7E). Our results demonstrate that the expression patterns of RhoJ and ERG within the heart are very similar. The expression levels are highest in endocardial ECs, followed by venous ECs, and are lowest in the capillary ECs.

Discussion

The molecular mechanisms that underlie EC cell lumen formation and tube assembly during vascular morphogenesis continue to emerge. Pioneering work in the 1990s demonstrated the critical role of Rho GTPases in mediating cytoskeletal signaling in the setting of cellular adhesion, migration, and regulation of cell-cell junctions.³⁴⁻³⁶ Subsequent studies have now helped to define a role for selected Rho GTPases in EC morphogenesis. In particular, the Rho GTPases Cdc42 and Rac1 are required for lumen formation, whereas RhoA is not.^{6,7} EC vacuoles accumulate directly adjacent to the centrosome in a region where Cdc42 and Rac1 levels are markedly increased.⁵ Our study supports a novel role for the Rho

family member RhoJ in EC morphogenesis and in particular in lumen formation. Suppression of RhoJ protein levels markedly inhibited EC lumen formation in 3D matrices. Furthermore, we have shown that RhoJ can coprecipitate with the highly related Rho GTPase family member Cdc42, suggesting that they may interact directly or with a common binding partner. In any case, it appears that they interact in a multicomponent complex that may be critical for proper EC lumen formation.²⁸ Finally, we observed that suppression of RhoJ leads to reciprocal effects on Rho GTPase activation with suppression of Rac1 activation and marked induction of RhoA activity. Our previous studies support a role for RhoA activation in EC lumen collapse and tube disassembly.³⁰ The exact mechanism by which suppression of RhoJ leads to RhoA activation remains to be determined.

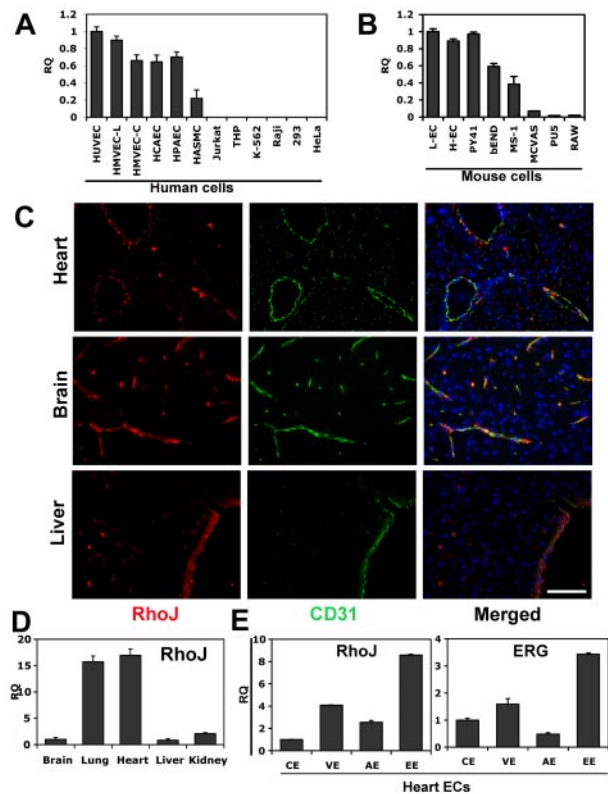


Figure 7. RhoJ expression is highly enriched in ECs. RNA was extracted from different cell types and QPCR was performed using RhoJ-specific primers ($n = 3$). (A) RhoJ expression in human ECs and non-ECs. The results are shown relative to HUVECs. Cells used include human ECs: HUVECs, HMVEC-Ls (human lung microvascular ECs), HMVEC-Cs (human cardiac microvascular ECs), HCAECs (human coronary artery ECs), HPAECs (human pulmonary artery ECs) and human non-ECs: HASMCs (human aortic smooth muscle cell ECs), Jurkat, THP, K-562, Raji, 293, and HeLa cells. (B) RhoJ expression in mouse ECs and non-ECs. Cells used include mouse primary ECs isolated from mouse lung (L-ECs) and heart (H-ECs), and the mouse EC cell lines MS-1, bEnd, PY41, and non-EC cell lines MCVAS (mouse smooth muscle cell), PU5, and RAW. The results are shown relative to L-ECs. (C) Representative images of immunofluorescent staining of RhoJ in mouse brain, liver, and heart. Tissues represent frozen sections stained for RhoJ (red), CD31 (green), or DAPI (blue). Magnification 40 \times . Scale bar indicates 75 μ m. (D) Examination of RhoJ expression in mouse tissues. RNAs were extracted from a variety of mouse tissues. cDNA were prepared from RNAs and used in QPCR. RhoJ expression was analyzed using RhoJ-specific primers and normalized against TBP ($n = 3$). The data are shown relative to brain. (E) Mouse heart was collected and sectioned, followed by H&E staining. ECs from different vascular beds were isolated using laser capture microdissection LMD. RNA was extracted and gene expression of RhoJ and ERG was analyzed by QPCR using specific primers. The data are presented as a ratio compared with VE-cadherin to normalize the EC numbers captured in LMD. EE indicates endocardial ECs; VE, venule ECs; AE, artery ECs; and CE, capillary ECs ($n = 3$).

RhoJ was first isolated by Vignal et al and was shown to be highly homologous to TC10 and Cdc42.³⁷ Northern blot analysis showed the highest expression of RhoJ in the heart and lung, with lesser amounts in the liver and brain. No analysis of cell-type specificity was conducted. In the same study, it was also shown that RhoJ interacts with WASP and Pak1.³⁷ Furthermore, overexpression of RhoJ in fibroblasts was associated with the production of numerous filopodia (> 30/cell) and a reduction in the actin stress fibers, which would be consistent with an effect of Cdc42 activation and RhoA inactivation, respectively. More recently, studies in HeLa cells have demonstrated that recombinantly expressed RhoJ is also a regulator of the early endocytic pathway.³⁸ RhoJ was shown to localize to the plasma membrane and to early endocytic compartments. Suppression of RhoJ in HeLa cells using siRNA directed against it did not affect receptor-dependent internalization of transferrin. However, transferrin accumulated in Rab5-positive uncoated endocytic vesicles and failed to reach the early endosome antigen-1–positive endosomal compartments and the pericentriolar recycling endosomes.

Of particular interest to us was the fact that, unlike other Rho GTPases, RhoJ appears to be unique in that its expression is enriched in ECs (Figure 7 and supplemental Figure 7), suggesting that it may have a particularly unique role with respect to EC function. Of the other Rho family members, only RhoB exhibited a somewhat EC-restricted pattern of expression, although some expression was observed in HEK293 and HeLa cells. Interestingly, RhoB-knockout mice exhibit defects in retinal vasculogenesis.³⁹ Furthermore, reduction of RhoB expression or activity using antisense or dominant-negative forms of the protein is associated with apoptosis in the sprouting ECs of newly formed vessels in neonatal rats.³⁹

Although considerable progress has been made with respect to the downstream effectors of the Rho GTPases, much less is known about the transcriptional regulation of these proteins. We have shown previously that Ets-1 regulates the expression of RhoC during the process of epithelial to mesenchymal transition.⁴⁰ Our study is the first to demonstrate a link between ETS factors and the transcriptional regulation of Rho GTPases in ECs. It is not entirely surprising that such a link might exist, given the fact that several

ETS factors have been implicated in the regulation of angiogenesis and vasculogenesis. Ets1 and Ets2 play overlapping roles during vascular development.⁴¹ Several ETS factors are highly enriched in the angiogenic blood vessels of tumors.⁴² In particular, Ets1 is a downstream target of several angiogenic factors, including VEGF and hepatocyte growth factor (HGF).⁴³ We have also shown that the ETS factor Elf-1 is up-regulated in embryonic and tumor blood vessels and that dominant-negative forms of Elf-1 can block tumor growth through inhibition of angiogenesis.⁴⁴ Future studies are needed to evaluate the role of ERG and RhoJ in EC morphogenesis during embryonic vascular development and in the setting of pathologic angiogenesis. In summary, our study demonstrates a novel role for the ETS factor ERG in the transcriptional regulation of the Rho GTPase RhoJ. Furthermore, our results strongly support a novel role of RhoJ in EC morphogenesis.

Acknowledgments

This work was supported by grants from the National Institutes of Health (PO1 HL76540 to P.O. and W.C.A and R01 HL59373 to G.E.D.) and from the American Heart Association (Established Investigator Award EIA0740012 to P.O.).

Authorship

Contribution: L.Y. performed the research, analyzed the data, designed the experiments, and wrote the manuscript; A.S., A.N.S., and S.S. performed the research and analyzed the data; A.L.B. and P.J.Z. performed the research; K.S. provided technical support; M.B. analyzed the data; J.A.N. designed the experiments and provided technical support; and G.M., W.C.A., G.E.D., and P.O. designed the experiments and wrote the manuscript.

Conflict-of-interest disclosure: The authors declare no competing financial interests.

Correspondence: Peter Oettgen, Research North RM 270D, Beth Israel Deaconess Medical Center, 330 Brookline Ave, Boston, MA 02115; e-mail: joettgen@caregroup.harvard.edu.

References

- Adams RH, Alitalo K. Molecular regulation of angiogenesis and lymphangiogenesis. *Nat Rev Mol Cell Biol*. 2007;8(6):464-478.
- Davis GE, Bayless KJ. An integrin and Rho GTPase-dependent pinocytotic vacuole mechanism controls capillary lumen formation in collagen and fibrin matrices. *Microcirculation*. 2003;10(1):27-44.
- Lubarsky B, Krasnow MA. Tube morphogenesis: making and shaping biological tubes. *Cell*. 2003;112(1):19-28.
- Iruela-Arispe ML, Davis GE. Cellular and molecular mechanisms of vascular lumen formation. *Dev Cell*. 2009;16(2):222-231.
- Davis GE, Koh W, Stratman AN. Mechanisms controlling human endothelial lumen formation and tube assembly in three-dimensional extracellular matrices. *Birth Defects Res C Embryo Today*. 2007;81(4):270-285.
- Bayless KJ, Davis GE. The Cdc42 and Rac1 GTPases are required for capillary lumen formation in three-dimensional extracellular matrices. *J Cell Sci*. 2002;115(pt 6):1123-1136.
- Koh W, Mahan RD, Davis GE. Cdc42- and Rac1-mediated endothelial lumen formation requires Pak2, Pak4 and Par3, and PKC-dependent signaling. *J Cell Sci*. 2008;121(pt 7):989-1001.
- Martin-Belmonte F, Gassama A, Datta A, et al. PTEN-mediated apical segregation of phosphoinositides controls epithelial morphogenesis through Cdc42. *Cell*. 2007;128(2):383-397.
- Martin-Belmonte F, Yu W, Rodriguez-Fraticelli AE, et al. Cell-polarity dynamics controls the mechanism of lumen formation in epithelial morphogenesis. *Curr Biol*. 2008;18(7):507-513.
- Koh W, Stratman AN, Sacharidou A, Davis GE. In vitro three dimensional collagen matrix models of endothelial lumen formation during vasculogenesis and angiogenesis. *Methods Enzymol*. 2008;443:83-101.
- Wasyluk B, Hahn SL, Giovane A. The Ets family of transcription factors. *Eur J Biochem*. 1993;211(1-2):7-18.
- Ijijn K, Dube A, Kontusaari S, et al. Role of ets factors in the activity and endothelial cell specificity of the mouse Tie gene promoter. *FASEB J*. 1999;13(2):377-386.
- Dube A, Akbarali Y, Sato TN, Libermann TA, Oettgen P. Role of the Ets transcription factors in the regulation of the vascular-specific Tie2 gene. *Circ Res*. 1999;84(10):1177-1185.
- Dube A, Thai S, Gaspar J, et al. Elf-1 is a transcriptional regulator of the Tie2 gene during vascular development. *Circ Res*. 2001;88(2):237-244.
- Karantzoulis-Fegaras F, Antoniou H, Lai SL, et al. Characterization of the human endothelial nitric oxide synthase promoter. *J Biol Chem*. 1999;274(5):3076-3093.
- Schwachtgen JL, Janel N, Barek L, et al. Ets transcription factors bind and transactivate the core promoter of the von Willebrand factor gene. *Oncogene*. 1997;15(25):3091-3102.
- Vlaeminck-Guillem V, Carrere S, Dewitte F, Stehelin D, Desbiens X, Duterque-Coquillaud M. The Ets family member Erg gene is expressed in mesodermal tissues and neural crests at fundamental steps during mouse embryogenesis. *Mech Dev*. 2000;91(1-2):331-335.
- Baltzinger M, Mager-Heckel AM, Remy P. XI erg: expression pattern and overexpression during development plead for a role in endothelial cell differentiation. *Dev Dyn*. 1999;216(4-5):420-433.
- Hewett PW, Nishi K, Daft EL, Clifford Murray J. Selective expression of erg isoforms in human endothelial cells. *Int J Biochem Cell Biol*. 2001;33(4):347-355.
- Yuan L, Nikolova-Krstevski V, Zhan Y, et al. Anti-inflammatory effects of the ETS factor ERG in

- endothelial cells are mediated through transcriptional repression of the interleukin-8 gene. *Circ Res*. 2009;104(9):1049-1057.
21. Birdsey GM, Dryden NH, Amsellem V, et al. Transcription factor Erg regulates angiogenesis and endothelial apoptosis through VE-cadherin. *Blood*. 2008;111(7):3498-3506.
 22. Liu J, Yuan L, Molema G, et al. Vascular bed-specific regulation of the von Willebrand factor promoter in the heart and skeletal muscle. *Blood*. 2011;117(1):342-351.
 23. Pimanda JE, Chan WY, Donaldson IJ, Bowen M, Green AR, Gottgens B. Endoglin expression in the endothelium is regulated by Fli-1, Erg, and Elf-1 acting on the promoter and a -8-kb enhancer. *Blood*. 2006;107(12):4737-4745.
 24. Nikolova-Krstevski V, Yuan L, Le Bras A, et al. ERG is required for the differentiation of embryonic stem cells along the endothelial lineage. *BMC Dev Biol*. 2009;9:72.
 25. McLaughlin F, Ludbrook VJ, Cox J, von Carlowitz I, Brown S, Randi AM. Combined genomic and antisense analysis reveals that the transcription factor Erg is implicated in endothelial cell differentiation. *Blood*. 2001;98(12):3332-3339.
 26. He X, Kuijpers GA, Goping G, et al. A polarized salivary cell monolayer useful for studying trans-epithelial fluid movement in vitro. *PLoS Arch*. 1998;435(3):375-381.
 27. Stratman AN, Schwindt AE, Malotte KM, Davis GE. Endothelial-derived PDGF-BB and HB-EGF coordinately regulate pericyte recruitment during vasculogenic tube assembly and stabilization. *Blood*. 2010;116(22):4720-4730.
 28. Sacharidou A, Koh W, Stratman AN, Mayo AM, Fisher KE, Davis GE. Endothelial lumen signaling complexes control 3D matrix-specific tubulogenesis through interdependent Cdc42- and MT1-MMP-mediated events. *Blood*. 2010;115(25):5259-5269.
 29. Lampugnani MG, Orsenigo F, Rudini N, et al. CCM1 regulates vascular-lumen organization by inducing endothelial polarity. *J Cell Sci*. 2010;123(pt 7):1073-1080.
 30. Bayless KJ, Davis GE. Microtubule depolymerization rapidly collapses capillary tube networks in vitro and angiogenic vessels in vivo through the small GTPase Rho. *J Biol Chem*. 2004;279(12):11686-11695.
 31. Bokoch GM. Biology of the p21-activated kinases. *Annu Rev Biochem*. 2003;72:743-781.
 32. Buckanovich RJ, Sasaroli D, O'Brien-Jenkins A, et al. Tumor vascular proteins as biomarkers in ovarian cancer. *J Clin Oncol*. 2007;25(7):852-861.
 33. Asgeirsdóttir SA, Kamps JA, Bakker HI, et al. Site-specific inhibition of glomerulonephritis progression by targeted delivery of dexamethasone to glomerular endothelium. *Mol Pharmacol*. 2007;72(1):121-131.
 34. Ridley AJ, Hall A. The small GTP-binding protein rho regulates the assembly of focal adhesions and actin stress fibers in response to growth factors. *Cell*. 1992;70(3):389-399.
 35. Ridley AJ, Hall A. Distinct patterns of actin organization regulated by the small GTP-binding proteins Rac and Rho. *Cold Spring Harb Symp Quant Biol*. 1992;57:661-671.
 36. Hall A, Paterson HF, Adamson P, Ridley AJ. Cellular responses regulated by rho-related small GTP-binding proteins. *Philos Trans R Soc Lond B Biol Sci*. 1993;340(1293):267-271.
 37. Vignal E, De Toledo M, Comunale F, et al. Characterization of TCL, a new GTPase of the rho family related to TC10 and Ccdc42. *J Biol Chem*. 2000;275(46):36457-36464.
 38. de Toledo M, Senic-Matuglia F, Salamero J, et al. The GTP/GDP cycling of rho GTPase TCL is an essential regulator of the early endocytic pathway. *Mol Biol Cell*. 2003;14(12):4846-4856.
 39. Adini I, Rabinovitz I, Sun JF, Prendergast GC, Benjamin LE. RhoB controls Akt trafficking and stage-specific survival of endothelial cells during vascular development. *Genes Dev*. 2003;17(21):2721-2732.
 40. Bellovin DI, Simpson KJ, Danilov T, et al. Reciprocal regulation of RhoA and RhoC characterizes the EMT and identifies RhoC as a prognostic marker of colon carcinoma. *Oncogene*. 2006;25(52):6959-6967.
 41. Oettgen P. Functional redundancy of Ets1 and Ets2. *Blood*. 2009;114(5):934-935.
 42. Oettgen P. The role of ets factors in tumor angiogenesis. *J Oncol*. 2010;2010:767384.
 43. Hashiya N, Jo N, Aoki M, et al. In vivo evidence of angiogenesis induced by transcription factor Ets-1: Ets-1 is located upstream of angiogenesis cascade. *Circulation*. 2004;109(24):3035-3041.
 44. Huang X, Brown C, Ni W, Maynard E, Rigby AC, Oettgen P. Critical role for the Ets transcription factor ELF-1 in the development of tumor angiogenesis. *Blood*. 2006;107(8):3153-3160.